*promoting access to White Rose research papers*

White Rose
Research Online

**Universities of Leeds, Sheffield and York**
**http://eprints.whiterose.ac.uk/**

This is an author produced version of a paper published in **Microelectronics Journal.**

White Rose Research Online URL for this paper:
http://eprints.whiterose.ac.uk/7928/

**Published paper**
Isic, G., Milanovic, V., Radovanovic, J., Indjin, D., Ikonic, Z. and Harrison, P. (2009) *Nonparabolicity effects and the spin-split electron dwell time in symmetric III-V double-barrier structures.* Microelectronics Journal, 40.

http://dx.doi.org/10.1016/j.mejo.2008.06.032

*White Rose Research Online*
*eprints@whiterose.ac.uk*

# Nonparabolicity effects and the spin-split electron dwell time in symmetric III-V double-barrier structures

G. Isić[1,*], V. Milanović[2], J. Radovanović[2], D. Indjin[1], Z. Ikonić[1] and P. Harrison[1]

[1]School of Electronic and Electrical Engineering, University of Leeds, Leeds LS2 9JT, United Kingdom

[2]School of Electrical Engineering, University of Belgrade, Bulevar kralja Aleksandra 73, 11120 Belgrade, Serbia

## Abstract

We start from the fourth order nonparabolic and anisotropic conduction band bulk dispersion relation to obtain an one-band effective Hamiltonian which we apply to an AlGaSb symmetric double-barrier structure with resonant energies significantly (more than 200meV) above the well bottom. The spin-splitting is described by the $k^3$ Dresselhaus spin-orbit coupling term modifying only the effective mass of the spin eigenstates in the investigated structure. Apart from the bulk-like resonant energy shift due to the band nonparabolicity, we obtain a substantial shift depending on the choice of boundary conditions for the envelope functions at interfaces between different materials. The shift of resonant energy levels leads to the change of spin-splitting and the magnitude of the dwell times. We attempt to explain the influence of both the nonparabolicity and boundary conditions choice by introducing various effective masses.

## 1. Introduction

Recently [1], a symmetric III-V heterostructure has been shown to exhibit spin-dependent transmission probabilities. Glazov et al. [2] have shown that the transmitted electrons generate a spin polarized current if an in-plane electric field is applied to a double-barrier resonant tunnelling structure (DB-RTS). In our previous work, we have discussed that significant spin-polarization may be expected in both asymmetric DB-RTSs and symmetric triple-barrier structures [3, 4] with the the influence of the perpendicular electric field proven to be particularly important. Spin filters based on all-semiconductor structures might never reach the performance of those based on ferromagnetic materials or diluted magnetic semiconductors, especially if care is taken to optimize the latter [5, 6]. However, all-semiconductor structures have some important virtues - better compatibility with the existing semiconductor technology and the prospect of achieving spin polarization even in the absence of magnetic fields.

Most of the theoretical work so far focused on spatial aspects of the spin filtering process (i.e. those corresponding to stationary states). A spin dynamic filter has been proposed in [7]. Using the electron dwell time as a well established parameter for studying the temporal aspects of double-barrier tunnelling [8, 9], we discuss the effects of the band nonparabolicity.

The spin-splitting in III-V semiconductors has its origins in the spin orbit coupling (SOC) and the inversion asymmetry of the zinc-blende structure so the spin eigenstates are determined by the wave vector. To avoid scattering between spin-split subbands, Ref. [2] introduces a DB-RTS in which the energy of the electrons is significantly above (more than 200meV) the conduction band (CB) bottom of the well region, suggesting that significant nonparabolicity and anisotropy effects might be expected.

## 2. The double-barrier resonant structure and nonparabolicity

In the absence of external electric and magnetic fields, the spin-splitting in symmetrical structures based on III-V semiconductors is described by the Dresselhaus $k^3$ Hamiltonian [1, 10] as

$$H_D = \gamma_0 \left[ \sigma_x k_x (k_y^2 - k_z^2) + \sigma_y k_y (k_z^2 - k_x^2) + \sigma_z k_z (k_x^2 - k_y^2) \right]. \tag{1}$$

$k_x$, $k_y$ and $k_z$ are the components of the wave vector **k**, $\sigma_x$, $\sigma_y$ and $\sigma_z$ are the Pauli spin matrices and the effective Hamiltonian is obtained by letting $k_z$=–id/dz. As pointed out by [1] for the single-barrier and by [2] for the double-barrier structure shown in Fig. 1., Eq. (1) is simplified to

$$H_D = (\sigma_x k_x - \sigma_y k_y) \frac{\mathrm{d}}{\mathrm{dz}} \gamma_0 \frac{\mathrm{d}}{\mathrm{dz}}, \tag{2}$$

since $|k_z|>>k_x$, $k_y$ for electrons with $E\approx E_{c0}$ (see Fig. 1.). The consequence is that the spin-state of electrons in either of the states described by the spinors

$$\chi_s = \frac{1}{\sqrt{2}}\begin{bmatrix} 1 \\ -s\exp(-i\varphi) \end{bmatrix}, \quad s = \pm, \tag{3}$$

is preserved in the tunnelling process described by the diagonalized spin-dependent effective Hamiltonian

$$H_s = \alpha_0 \frac{d^4}{dz^4} - \frac{\hbar^2}{2M_s}\frac{d^2}{dz^2} + E(k_{\|},\varphi)\,. \tag{4}$$

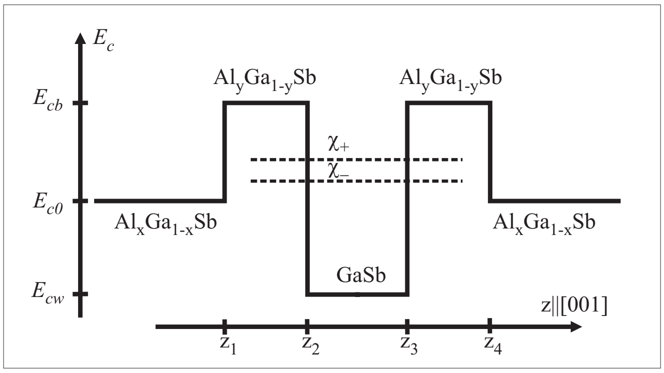

Fig. 1. The symmetrical double-barrier resonant tunnelling structure.
Structure parameters: $x\approx0.15$, $y\approx0.3$, $z_1=0$, $z_2=50$A, $z_3=75$A, $z_4=125$A, $E_{cb}=750$meV, $E_{c0}=200$meV, $E_{cw}=0$, $m_e=m_c=0.065m_0$, $m_b=0.073m_0$, $m_w=0.057m_0$, $\alpha_{0e}=\alpha_{0c}=-1310$eVA$^4$, $\alpha_{0b}=-1129$eVA$^4$, $\alpha_{0w}=-1493$eVA$^4$, $\beta_{0e}=\beta_{0c}=-1143$eVA$^4$, $\beta_{0b}=-1070$eVA$^4$, $\beta_{0w}=-1215$eVA$^4$, $\gamma_{0e}=\gamma_{0c}=157$eVA$^3$, $\gamma_{0b}=129$eVA$^3$, $\gamma_{0w}=185$eVA$^3$.

The Dresselhaus constant, $\gamma_0$, in (2) is defined as positive so that $\chi_+$ state has a slightly higher energy than the $\chi_-$ state in the corresponding bulk dispersion. Eq. (4) is obtained from the fourth order bulk dispersion for the conduction band [11]

$$E(k) = \frac{\hbar^2k^2}{2m} + \alpha_0 k^4 + \beta_0\left(k_x^2k_y^2 + k_y^2k_z^2 + k_z^2k_x^2\right) + s\gamma_0 k_z^2\sqrt{k_x^2+k_y^2}\,, \tag{5}$$

so that $k_x=k_{\|}\cos\varphi$, $k_y=k_{\|}\sin\varphi$,

$$\frac{1}{M_s} = \frac{1}{m} + \frac{2}{\hbar^2}\left(s\gamma_0 k_{\|} + (2\alpha_0+\beta_0)k_{\|}^2\right), \tag{6}$$

and

$$E(k_{\|},\varphi) = E_c + \left(\alpha_0 + \beta_0\frac{\sin^2 2\varphi}{4}\right)k_{\|}^4 + \frac{\hbar^2k_{\|}^2}{2m}\,. \tag{7}$$

We have assumed that the effective mass, $m$, the nonparabolicity coefficient, $\alpha_0$, the anisotropy coefficient, $\beta_0$ and the Dresselhaus constant, $\gamma_0$ vary along the structure but are constant inside the individual layers (see Fig. 1.). The assumption of different parameter values in the layers is somewhat arbitrary. We have used it to emphasize the boundary conditions issue. Apart from $\gamma_0$ obtained from [12], we have investigated the values for these coefficients for the AlGaSb system within three bulk dispersion models and used linear interpolation to obtain the values of alloy parameters.

'Model a)' is a 14-band kp model described by [13] and [14] which has previously been used for AlGaAs systems. We have calculated the values for $\alpha_0$ and $\beta_0$ for AlSb and GaSb using the theory from [13, 14] and the parameters from [12].

'Model b)' is a higher order nonparabolic but isotropic dispersion relation for the conduction band given in [15] which has been obtained by fitting the theoretical expressions for the imaginary part of the dielectric function ε [16] to the experimental values obtained from various sources.

'Model c)' represents the fit of the dispersion formula (5) to the bulk dispersion of AlSb and GaSb which we obtained by pseudopotential calculations.

Fig. 2. shows the dispersion curves corresponding to these models and the parabolic curve. We have chosen to use the values of $m$, $\alpha_0$ and $\beta_0$ obtained from the 'Model c)'. It is seen from Fig. 2. that 'Model c)' and 'Model b)' agree fairly well, whereas the nonparabolicity predicted by 'Model a)' appears to be an overestimate. The energy range we were interested in is 200-400meV, (see Fig. 1.).

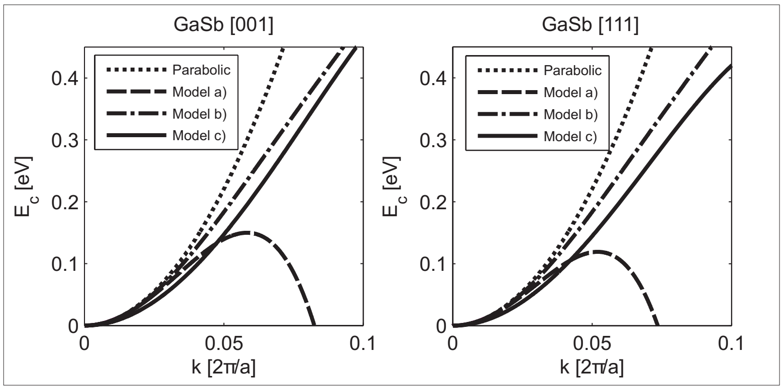

Fig. 2. Comparison of various models considered for modelling the transmission characteristics of the DB-RTS from Fig. 1. These are the GaSb bulk dispersion curves. For the AlSb bulk dispersion, similar results apply.

The equienergy curves in the ($k_x$, $k_y$) plane shown in Fig. 3. demonstrate that the conduction band anisotropy may indeed be neglected (the same applies to AlSb), even in the case of using the value of $\beta_0$ from 'Model a)' which is an order of magnitude higher than the one predicted by the 'Model c)'.

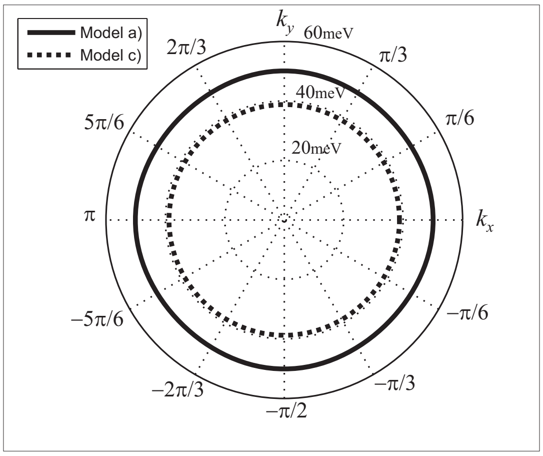

Fig. 3. The in-plane ($k_x$,$k_y$) anisotropy of the conduction band in GaSb for $k_{||}=0.025\cdot 2\pi/a$ with:
'Model a)' paramerers: $m=0.041m_0$, $\alpha_0=-11696\text{eVA}^4$, $\beta_0=-9059\text{eVA}^4$ and
'Model c)' parameters: $m=0.057m_0$, $\alpha_0=-1493\text{eVA}^4$, $\beta_0=-1215\text{eVA}^4$.
In both 'Model a)' and 'Model c)' the anisotropy is negligible.

The spin-dependent wave functions, $\psi_s$, are obtained by solving

$$H_s\psi_s = E\psi_s\,. \tag{8}$$

These represent linear combinations of momentum eigenstates, $\exp(ik_{z,s})$ and $\exp(-ik_{z,s})$, in each individual layer connected by the boundary conditions at interfaces $z_1$, $z_2$, $z_3$ and $z_4$. The values of $k_{z,s}$ in the layers for an electron with given $E$, $k_x$ and $k_y$ are obtained in a straightforward manner by excluding the two spurious solutions among the four solutions of the quartic equation. The spin-dependent reflection, $R_s$, and transmission, $T_s$, coefficients are defined so that

$$\psi_s = \exp(ik_{z,s}z) + R_s\exp(-ik_{z,s}z), \qquad z < z_1 \tag{9}$$

and

$$\psi_s = T_s \exp(ik_{z,s}z), \quad z > z_4, \tag{10}$$

with resonant energies, $E_{R,s}$, having the unit trasmission probability,

$$\left|T_s(E_{R,s})\right| = 1. \tag{11}$$

Since (8) is a fourth order equation and only two of four solutions for $k_{z,s}$ are physically meaningful (so only two linearly independent conditions are allowed), (8) cannot be satisfied in every point, i.e. the boundary conditions need to be imposed artificially. We do not introduce any criteria for the suitability of particular boundary conditions (such as models of higher accuracy or experimental results), but carry out the calculations for three different boundary conditions and show how sensitive the results are on the particular choice. To define the boundary conditions, we introduce two additional parameters with the dimension of mass.

For a momentum eigenstate, $\exp(ik_{z,s})$, (4) and (8) give

$$E = \frac{\hbar^2 k_{z,s}^2}{2m_{H,s}} + E_{\|}(k_{\|},\varphi), \tag{12}$$

where we have introduced the mass $m_{H,s}$ by

$$\frac{1}{m_{H,s}} = \frac{2\alpha_0 k_{z,s}^2}{\hbar^2} + \frac{1}{M_s}. \tag{13}$$

This is the 'local' effective mass along $k_z$. Next, consider the mass, $m_{J,s}$, given by

$$\frac{1}{m_{J,s}} = \frac{4\alpha_0 k_{z,s}^2}{\hbar^2} + \frac{1}{M_s} = \frac{1}{\hbar^2}\frac{1}{k_{z,s}}\frac{\partial E}{\partial k_{z,s}}. \tag{14}$$

We define the boundary conditions as

$$\psi_s(z_n^-) = \psi_s(z_n^+) \text{ and } \frac{1}{C_s}\frac{d\psi_s}{dz}(z_n^-) = \frac{1}{C_s}\frac{d\psi_s}{dz}\psi_s(z_n^+), \tag{15}$$

for $n$=1,2,3,4 while Cs is set to $m_{J,s}$, $m_{H,s}$ or $M_s$. In the next section, we will investigate the influence of the choice of boundary conditions by changing the way $C_s$ are defined. The importance of $m_{J,s}$ comes from the fact that by putting $C_s$=$m_{J,s}$ the current density probability is preserved.

The dynamics of the spin-dependent DB-RTS tunnelling [7, 9] is investigated by introducing the electron dwell time with

$$\tau_{D,s} = \frac{\int_{z_1}^{z_4} |\psi_s| dz}{J_{in,s}}, \tag{16}$$

where $J_{in,s}$ is the probability current density of the incoming electron with spin $s$ which equals the overall probability current density $J_s$ if the transmission equals unity.

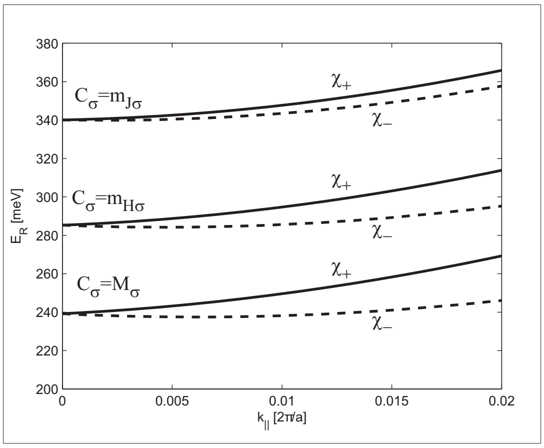

Fig. 4. Dependence of the spin-split resonance energies $E_{R,s}$ on the choice of boundary conditions. These results are for the $\chi_+$ and $\chi_-$ states. The spin of an arbitrary state, $a_+\chi_+ + a_-\chi_-$, is not conserved in the tunnelling process.

The extent to which a physical meaning may be ascribed to the dwell time is arguable (see e.g. [8] and [17]), but it clearly gives a good starting point for estimating the time scale of the tunnelling process and, hence, it is interesting for studying the spin-splitting in the time domain.

## 3. Numerical results and discussion

We have found that the band nonparabolicity introduces a bulk-like displacement of the resonant energy levels $E_{R,s}$, the magnitude of which is ~100meV as can be estimated from Fig. 2. Varying the boundary conditions introduces similar effects to the resonant states, affecting the position of $E_{R,s}$. In Fig. 4. the dependence of $E_{R,s}$ on $k_{\|}$ is shown for three different boundary conditions. We see that as the mass-like parameter is appearing in (15) is increased from $m$ to $m_{H,s}$ and, finally, to $m_{J,s}$ (because $\alpha_0$ is negative and $k_{z,s}$ is real in the well) the position of the resonant energy levels is increased, contrary to the expected decrease. A similar effect is observed by 'turning on' the nonparabolicity, i.e. although the 'local' effective mass in the nonparabolic model is higher than $m$, the resonant energy levels are increased. Ref. [11] reported the same ('nonintuitive') result of the increase of confinement energies in quantum well structures when nonparabolicity is taken into account. All the three boundary conditions are reduced to the usual BenDaniel-Duke boundary conditions in the limit $\alpha_0$, $\beta_0 \rightarrow 0$. However, for nonzero $\alpha_0$, $\beta_0$, only the $Cs=m_{J,s}$ condition yields the conservation of current density probability.

The dependence of the spin-splitting, $E_{R,+}-E_{R,-}$, on the choice of $C_s$ shown on Fig. 4. is mainly due to the displacement of $E_{R,s}$, as well. If we assume that the position of $E_{R,s}$ is an approximately linear function of the effective mass, and the two spin states have a fixed (determined by bulk properties) diference of the inverse of their effective masses, we can explain the decrease of the splitting observed in Fig. 4.

To discuss the variation of the magnitude of $\tau_D$ for the resonant energy levels, we note that [8]

$$\tau_D = \hbar / \Gamma , \tag{17}$$

where $\Gamma$ is the width of the transmission resonance i.e. the energy uncertainty of the resonant quasibound state. This quantity is clearly increased as $E_{R,s}$ is increased since an electron in the barrier can interact with the environment behind the barriers more easily if its energy is higher. Therefore, $\tau_D$ is decreased as $E_{R,s}$ goes up. This reasoning is confirmed by our results shown in Fig. 5.

We have compared the results of our model with the results given in [9] and found excellent agreement when $\alpha_0$, $\beta_0 \rightarrow 0$. Taking into account the nonparabolicity changes the results but their order of magnitude remains the same.

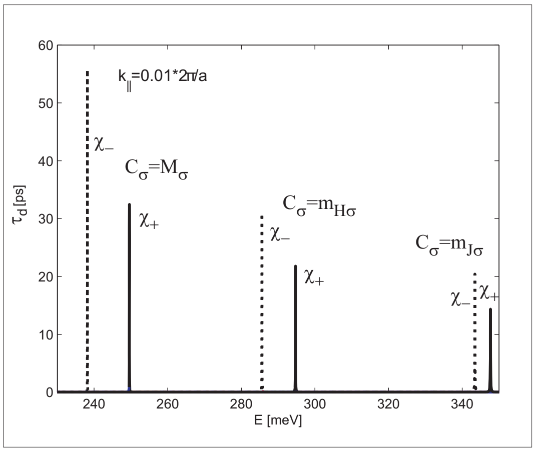

Fig. 5. The dwell time for various boundary conditions. The decrease of $\tau_D$ for increasing energies is explained by the increase of the energy uncertainty for quasibound states with higher energy.

In summary, we have carried out an analysis of nonparabolicity effects in a fourth-order one-band effective Hamiltonian model. The results indicate that including band nonparabolicity may substantially shift the resonant energy levels which is followed by 'secondary' effects, such as decrease of spin-splitting with the increase of the effective mass (due to the nonparabolicity or varying boundary conditions) and the decrease of dwell times. We have proven that the results are very sensitive even to the choice of boundary conditions alone, the issue of which exists even in parabolic models. The models which we studied, had a negligible band anisotropy. Our study of the GaSb and AlSb dispersion indicates that the 14-band kp model for calculating higher order $k$ terms in the conduction band dispersion, might not be appropriate for energies more than 100meV above the conduction band bottom.

## Acknowledgments

We acknowledge support from the NATO - Collaborative Linkage Grant 983316, the Serbian Ministry of Science and EPSRC (UK). G.I. acknowledges support from ORSAS in the U.K. and the University of Leeds.

*Corresponding author: elgi@leeds.ac.uk

## References

[1] V. I. Perel', S. A. Tarasenko, I. N. Yassievich, S. D. Ganichev, V. V. Belkov, and W. Prettl, Phys. Rev. B **67**, 201304 (2003).
[2] M. M. Glazov, P. S. Alekseev, M. A. Odnoblyudov, V. M. Chistyakov, S. A. Tarasenko, and I. N. Yassievich, Phys. Rev. B **71**, 155313 (2005).
[3] J. Radovanović et al. Opt. Mater. (2007), doi:10.1016/j.optmat.2007.05.037
[4] G. Isić, J. Radovanović, V. Milanović J. Appl. Phys. **102**, 123704 (2007).
[5] J. Radovanović, V. Milanović, Z. Ikonić, and D. Indjin, J. Appl. Phys. **99**, 073905 (2006).
[6] J. Radovanović, V. Milanović, Z. Ikonić, and D. Indjin, J. Phys. D: Appl. Phys. **40**, 5066 (2007).
[7] R. Romo and S. E. Ulloa, Phys. Rev. B **72** 121305 (2005).
[8] H. Mizuta and T. Tanoue, The Physics and Applications of Resonant Tunnelling Diodes, Cambridge University Press (1995).
[9] W. Li and Y. Guo, Phys. Rev. B **73**, 205311 (2006).
[10] G. Dresselhaus, Phys. Rev. **100**, 580 (1955).
[11] U. Ekenberg, Phys. Rev. B **40** 7714 (1989).
[12] J. -M. Jancu, R. Scholz, E. A. de Andrada e Silva, G. C. La Rocca, Phys. Rev. B **72**, 193201 (2005).
[13] U. Rossler, Solid State Commun. **49**, 943 (1984).
[14] M. Braun, U. Rossler, J. Phys. C **18**, 3365 (1985).
[15] S. Shokhovets, O. Ambacher, G. Gobsch, Phys. Rev. B **76**, 125203 (2007).
[16] S. Shokhovets, G. Gobsch, and O. Ambacher, Phys. Rev. B **74**, 155209 (2006).
[17] M. Tsuchiya, T. Matsusue, and H. Sakaki, Phys. Rev. Lett. **59**, 2356 (1987).